ELSEVIER

Journal of Fluids and Structures 19 (2004) 607–619

JOURNAL OF FLUIDS AND STRUCTURES

www.elsevier.nl/locate/jnlabr/yjfls

Equivalent linear modal parameter estimation for a nonlinear aeroelastic system

C.C. Marsden, S.J. Price*

Department of Mechanical Engineering, McGill University, Montréal, Québec, Canada H3A 2K6

Received 18 September 2003; accepted 16 March 2004

Abstract

A nonlinear dynamic system modal analysis methodology is applied to a two degree-of-freedom, nonlinear aeroelastic system. Modal analysis is an essential tool in the flight flutter testing of new and modified aircraft structures, and is used to identify system modal parameters such as frequency and damping. Traditional spectral methods based on the fast Fourier transform, rely on the assumption of system linearity. It has been shown that even isolated nonlinearities in the aircraft structure can contribute to errors in the estimated values of frequency and damping obtained from such a modal analysis. The reverse multiple-input/single-output method, described by Bendat, is a spectral analysis technique applicable to the frequency response function obtained from a nonlinear dynamical system. The technique uses a band-limited random forcing input to obtain the system response and permits the separation of the linear and nonlinear portions of the frequency response function within the frequency domain. The linear portion of the frequency response may then be used to recover the values of frequency and damping for the equivalent linear system. Results are presented for the application of this method to the specific case of a two degree-of-freedom, structurally nonlinear, aeroelastic system. It is shown that the method may be used to successfully recover the linear frequency response function using the input and output data for the nonlinear system.

1. Introduction

Modal testing is often employed in the determination of natural frequencies and damping levels in aircraft structures. In the forced response analysis, an exciting force is applied at a specified frequency or range of frequencies and the response of the system is measured. The frequency response function is obtained from the input and output time-history data, and then analysed to find the natural frequencies, mode shapes and damping values for the aeroelastic system. These parameters can be used to predict the responses to various excitations and to improve the dynamic behaviour of the system through design modification. Based on the linear model, the damping of the critical mode will increase with increasing airspeed and then decrease quite suddenly near the flutter speed. Depending on the specific combination of aeroelastic parameters, this decrease in damping can be quite sudden. At low values of damping, such as those associated with the onset of flutter, there is considerable uncertainty in the experimental measurement and determination of damping values. In aircraft flutter testing, potentially dangerous flight regimes are avoided by obtaining modal damping and frequency values at airspeeds well below the flutter speed and extrapolating the data to estimate the airspeed at which the onset of flutter instabilities is expected to occur. Natural frequency and damping

*Corresponding author.
E-mail address: stuart.price@mcgill.ca (S.J. Price).

0889-9746/$ - see front matter
doi:10.1016/j.jfluidstructs.2004.03.002

Nomenclature

a_h	nondimensional distance measured from the airfoil mid-chord to the elastic axis
b	airfoil semi-chord
c_h	translational viscous damping coefficient in plunge
c_α	torsional viscous damping coefficient in pitch
c_β	nondimensional distance of the flap hinge from the airfoil mid-chord
h	plunge displacement of the airfoil
I_α	moment of inertia of the airfoil/flap about the elastic axis
K_h	linear structural stiffness in plunge
K_α	linear structural stiffness in pitch
m	the combined aileron/flap mass per unit span
m_β	the flap mass per unit span
m_0	restoring moment preload for bilinear spring
r_α	nondimensional radius of gyration of the airfoil/flap about the elastic axis
U	nondimensional free stream velocity, $V/b\omega_\alpha$
U^*	nondimensional linear flutter velocity
V	free stream velocity
x_α	nondimensional distance from the airfoil center of mass to the elastic axis
x_β	nondimensional distance from the flap centre of mass to the flap hinge
α	pitch rotation of the airfoil, measured about the elastic axis
α_f	α at the start of the freeplay region
β	angular rotation of flap about flap hinge
δ	length of the bilinear stiffness freeplay region
ζ_α	viscous damping ratio in pitch, $c_\alpha/2I_\alpha\omega_\alpha$
ζ_ξ	viscous damping ratio in plunge, $c_h/2m_\alpha\omega_\alpha$
μ	airfoil-air mass ratio $m/\pi\rho b^2$
ξ	nondimensional plunge displacement, h/b
τ	nondimensional time, tV/b
ϖ_ξ	uncoupled frequency ratio, $\omega_\eta/\omega_\alpha$

values obtained at airspeeds as low as 50% of the linear flutter speed can be used to predict critical airspeeds using methods such as the flutter margin (Zimmerman and Weissenburger, 1964).

In the modal analysis, the structure is typically assumed to be linear and the parameters to be time-invariant. The frequency response function describes how the linear system responds to excitations at different frequencies, and is used to calculate modal damping values. The calculation of the frequency response function is based on the fact that a sinusoidal input to a linear system gives rise to a sinusoidal output at the same frequency as the input, although not necessarily at the same amplitude or in phase with it. Nonlinear dynamical systems respond to applied excitation differently from linear systems. Nonlinearities in aeroelastic systems can arise from both structural and aerodynamic sources and may initiate aeroelastic instabilities both above and below the flutter speed predicted by linear theory (Dowell and Tang, 2002). Typical nonlinear responses include limit cycle oscillations or in some cases, chaotic response. The study of nonlinear aeroelasticity presents many challenges and current research focuses on a number of different aspects of the problem (Dowell et al., 2003; Lee et al., 1999). In particular, the nonlinear response of a structurally nonlinear airfoil in subsonic flow has been the subject of a number of investigations, including experimental/theoretical correlations for both discontinuous (Conner et al., 1997, Tang et al., 1998) and continuous (O'Neil and Strganac, 1998; Sheta et al., 2002) structural nonlinearities.

One characteristic feature of nonlinear systems is that a single frequency excitation, such as a sinusoid, produces a multi-frequency response. In the case of a nonlinear mechanical system, a sinusoidal input will generate a response (generally small) at multiples, or super-harmonics, of the excitation frequency. In the case of a random or transient input, the frequency content of the nonlinear response can be more complex. A second important difference between the linear and nonlinear system responses concerns the frequency response function. For a linear system, the frequency response function at a given frequency is independent of the excitation signal used to obtain it—a random input and a sine-sweep across the same range of frequencies will produce the same frequency response function (provided the sine-sweep is done sufficiently slowly). In the case of the nonlinear system, the nonlinear frequency response can result in

distortions to the frequency response curve, and the distortion is different for different inputs. For the same nonlinear system, the frequency response function obtained for a sinusoidal, a multi-frequency sine-sweep, and a random input will not be the same. This can be an important result in modal analysis because where a linear system can be identified with one unique frequency response function, the equivalent nonlinear system cannot.

Both of the above nonlinear characteristics may be evident in systems that contain only slight nonlinearities. In the case of an aeroelastic system, it has been shown (Tang and Dowell, 1993) that the introduction of a limited structural nonlinearity in one degree-of-freedom of a two-degree-of-freedom aeroelastic system can cause distortion of the frequency response to a sine-sweep input. It has also been shown that this distortion can contribute to errors in the values of modal damping and frequency obtained from the frequency response function (Marsden and price, 2001). These results establish the motivation for attempting to extract the linear modal parameters from the nonlinear system frequency response function. Nonlinear dynamics theory presents a number of techniques for the analysis of nonlinear time series that may be applied to the aeroelastic system such as wavelets (Staszewski and Cooper, 2002), neural networks (Lee and Wong, 1998), and phase–space reconstruction (Alighanbari and Lee, 2003).

In this paper, the reverse multiple-input/single-output technique for the analysis and identification of nonlinear systems, developed by Bendat (1997) is used to separate the linear and the nonlinear content of the frequency response function before using the linear curve to recover the modal parameters. The particular system used to evaluate this approach is a two-degree-of-freedom aeroelastic system with a limited structural nonlinearity in the pitch degree-of-freedom. It is shown that this technique may be successfully applied to recover the linear portion of the frequency response from the total nonlinear response.

2. Problem modelling

2.1. Aeroelastic system model

The structural contribution to the aeroelastic model consists of a typical two-dimensional section with three degrees-of-freedom as shown in Fig. 1. The airfoil is rigid and free to move in both the bending and pitch directions, while the flap is constrained to move only as required in order to apply the forcing input to the system. The airfoil structural flexibility is provided by torsional and translational springs in the pitch and heave directions, respectively, while the flap has infinite stiffness and cannot respond to any of the forces to which it is exposed. The aerodynamic model is linear using incompressible, inviscid and unsteady flow, and is limited to small amplitude oscillations about the equilibrium position.

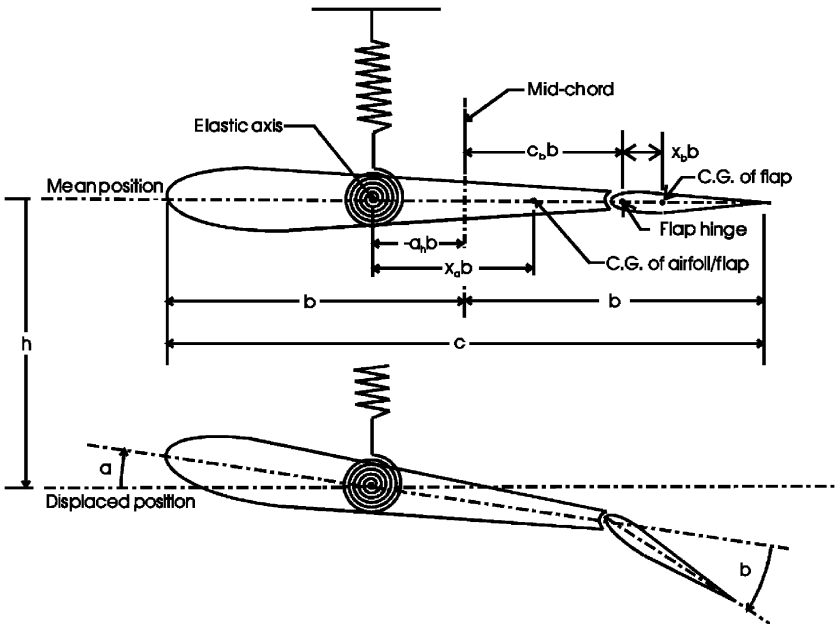

Fig. 1. Schematic of airfoil model.

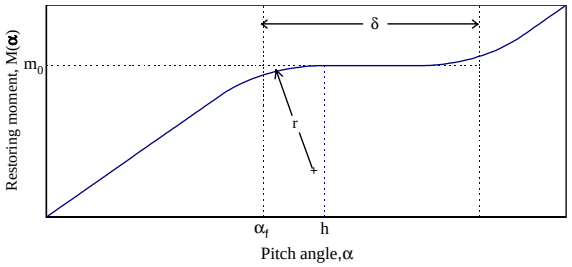

Fig. 2. Schematic of nonlinear restoring moment in pitch degree-of-freedom.

A limited structural nonlinearity is introduced in the form of a bilinear torsional stiffness in the pitch direction. This type of nonlinearity is sometimes employed in aeroelastic analyses to represent a worn or loose control surface hinge. In this study, the particular case of a bilinear nonlinearity with zero central stiffness is investigated. This type of nonlinearity is often called freeplay or backlash, and the freeplay region may have preload ($m_0 \neq 0$) or no preload ($m_0 = 0$). The dimension of the freeplay region within the nonlinear torsional spring (δ) is chosen to be sufficiently large to allow the nonlinear presence to distort the system response, but not to overwhelm the "linear" shape of the resulting frequency response curve. The result is not a highly nonlinear system, and permits an investigation into the impact of an isolated nonlinearity within a system that is "globally" linear. The particular nonlinear restoring force, $M(\alpha(\tau))$, used in this study is shown in Fig. 2 and may be described by the following equation:

$$M(\alpha(\tau)) = \begin{cases} M_0 + \alpha(\tau) - \alpha_f, & \text{for } \alpha \le \frac{\sqrt{2}}{2}\mathrm{h} - \left(1 + \frac{\sqrt{2}}{2}\right)\delta; \\ M_0 - r + \sqrt{r^2 - (\alpha(\tau) - h)^2}, & \text{for } \frac{\sqrt{2}}{2}h - \left(1 + \frac{\sqrt{2}}{2}\right)\delta < \alpha(\tau) < -h; \\ M_{0,} & \text{for } -h \le \alpha(\tau) \le h; \\ \mathrm{M}_0 + r - \sqrt{r^2 - (\alpha(\tau) - h)^2}, & \text{for } h < \alpha(\tau) < \left(1 + \frac{\sqrt{2}}{2}\right)\delta - \frac{\sqrt{2}}{2}h; \\ \alpha(\tau) - \alpha_f - \delta + M_0, & \text{for } \alpha(\tau) \ge \left(1 + \frac{\sqrt{2}}{2}\right)\delta - \frac{\sqrt{2}}{2}h. \end{cases} \tag{1}$$

The nondimensionalized equations of motion, obtained from Fung (1955) and modified to incorporate the nonlinear spring in the pitch degree-of-freedom, are given below:

$$\left(1 + \frac{1}{\mu}\right)\xi''(\tau) + \left(x_\alpha - \frac{a_h}{\mu}\right)\alpha''(\tau) + \left(\frac{m_\beta}{m}x_\beta - \frac{T_1}{\mu\pi}\right)\beta''(\tau) + \frac{1}{\mu}\alpha'(\tau) + 2\zeta_\xi\frac{\bar{\omega}_\xi}{U}\xi'(\tau) - \frac{T_4}{\mu\pi}\beta'(\tau) + \left(\frac{\bar{\omega}_\xi}{U}\right)^2\xi(\tau) = -\frac{2}{\mu}\left\{C_1\phi(\tau) + \int_0^\tau \phi(\tau - \sigma)\lambda(\sigma)d\sigma\right\}, \tag{2}$$

$$\left(\frac{x_\alpha}{r_\alpha^2} - \frac{a_h}{\mu r_\alpha^2}\right)\xi''(\tau) + \left(1 + \frac{1}{8\mu r_\alpha^2} + \frac{a_h^2}{\mu r_\alpha^2}\right)\alpha''(\tau) + \left(\frac{r_\alpha^2}{r_\beta^2} + \left[\frac{m_\beta}{m}\frac{x_\beta}{r_\alpha^2}(c_\beta - a_h)\right] - \frac{\left[T_7 + \{c_\beta - a_h\}T_1\right]}{\mu\pi r_\alpha^2}\right)\beta''(\tau) + \left(\frac{2\zeta_\alpha}{U} + \frac{(0.5 - a_h)}{\mu r_\alpha^2}\right)\alpha'(\tau) + \frac{1}{\mu\pi r_\alpha^2}(T_1 - T_8 - [c_\beta - a_h]T_4 + 0.5T_{11})\beta'(\tau) + \frac{(T_4 + T_{10})}{\mu\pi r_\alpha^2}\beta(\tau) + \frac{M(\alpha)}{U^2} = \frac{2}{\mu r_\alpha^2}(0.5 + a_h)\left[C_1\phi(\tau) + \int_0^\tau \phi(\tau - \sigma)\lambda(\sigma)d\sigma\right]. \tag{3}$$

Eq. (2) is for the bending, or plunge degree-of-freedom, and Eq. (3) is for the pitch direction.In the above equations, ϕ represents Wagner's function and, when solving the equations numerically, is replaced with the approximation given by Jones (1940),

$$\phi(\tau) = 1 - 0.165\mathrm{e}^{-0.0455\tau} - 0.335\mathrm{e}^{-0.3\tau}.$$

A "quasi-random" excitation is applied to the system by constraining the flap motion to oscillate according to a specified schedule given by the following equation:

$$\beta(\tau) = \beta_0 \sum_{i=1}^{500} \sin(\omega_i \tau),$$

where ω_i is a random frequency between 0.01 and 1.0 rad/nondimensional second. The power spectrum of this input function approximates a flat signal with a frequency content band-limited between 0.1 and 1.0 rad/nondimensional second. The range of frequencies is chosen in order to include both of the aeroelastic system natural frequencies.

The aeroelastic equations (2) and (3) contain integral terms on the right-hand side, introduced by the unsteady aerodynamic theory, and may not be solved directly using standard numerical methods for ordinary differential equations. In this study, the equations are reformulated as a set of eight ordinary differential equations using a technique developed by Alighanbari and Price (1996). The resulting system of eight first order differential equations is as given below:

$$[A]\{X'\} + [B]\{X\} = \{F\}, \tag{4}$$

where

$$\{X\} = \{x_1, x_2, x_3, x_4, x_5, x_6, x_7, x_8\}^{\mathrm{T}},$$

$$\{F\} = \{0, 0, 0, 0, 0, 0, f_1(\tau), f_2(\tau)\}^{\mathrm{T}},$$

$$[A] = \begin{bmatrix} 1 & 0 & 0 & 0 & 0 & 0 & 0 & 0 \\ 0 & 1 & 0 & 0 & 0 & 0 & 0 & 0 \\ 0 & 0 & 1 & 0 & 0 & 0 & 0 & 0 \\ 0 & 0 & 0 & 1 & 0 & 0 & 0 & 0 \\ 0 & 0 & 0 & 0 & 1 & 0 & 0 & 0 \\ 0 & 0 & 0 & 0 & 0 & 1 & 0 & 0 \\ 0 & 0 & 0 & 0 & 0 & 0 & m_1 & m_2 \\ 0 & 0 & 0 & 0 & 0 & 0 & n_1 & n_2 \end{bmatrix}$$

and

$$[B] = \begin{bmatrix} 0 & 0 & -1 & 0 & 0 & 0 & 0 & 0 \\ 0 & 0 & 0 & -1 & 0 & 0 & 0 & 0 \\ 0 & 0 & 0 & 0 & -1 & 0 & 0 & 0 \\ 0 & 0 & 0 & 0 & 0 & -1 & 0 & 0 \\ 0 & 0 & 0 & 0 & 0 & 0 & -1 & 0 \\ 0 & 0 & 0 & 0 & 0 & 0 & 0 & -1 \\ m_{13} & m_{14} & m_{10} & m_{11} & m_7 & m_8 & m_4 & m_5 \\ m_{13} & n_{14} & n_{10} & n_{11} & n_7 & n_8 & n_4 & n_5 \end{bmatrix},$$

where $f_1(\tau), f_2(\tau), m_1$ through m_{14}, and n_1 through n_{14}, are given in Appendix A.

2.2. Simulation of airfoil response

Eq. (4) is solved to obtain time histories of the airfoil motion in both the bending and pitch directions using a fourth-order Runge–Kutta numerical subroutine. The time step for the numerical integration was chosen to provide smooth derivatives up to the fourth order throughout the nonlinear region of the torsional spring. A more complete description of the methodology employed and results obtained is given in Marsden (2000). Time-history data records were obtained at a number of different airspeeds for the flap, pitch and plunge displacements. Each of the individual records is divided into 32 separate data records for the purpose of the Fourier ensemble-averaging. The length of the individual data records is 800 nondimensional seconds and determines the frequency resolution of the Fourier analysis. The time resolution interval between sample values within the data records is every 125 points generated by the numerical integration, or 0.391 nondimensional seconds. The choice of record length and time-resolution interval

results in a Nyquist cutoff frequency of 2.0 radians/second and a frequency resolution of 0.008 radians/nondimensional second.

2.3. The linear system

The equivalent linear system may also be described by equations (2) and (3), except that the expression for $M(\alpha(\tau))$ given in equation (1) is replaced by $M(\alpha(\tau)) = \alpha(\tau)$.

Frequency response curves for the linear system at a number of different airspeeds were obtained analytically from the Fourier-domain representation of the original equations of motion. The linear analysis provides a baseline against which the nonlinear results are compared.

3. The reverse multiple-input/single-output method for nonlinear system analysis

The separation of the linear and the nonlinear portions of the frequency response function may be accomplished using the reverse multiple-input/single-output method of analysis (Bendat, 1997). The reversal of the system input and output eliminates the feedback loop resulting from the nonlinear restoring moment in the pitch direction. The re-definition of the single output as two individual inputs permits the isolation of the linear and nonlinear contributions to the system response.

3.1. Method description

The two-degree-of-freedom aeroelastic system presented above may be reformulated as two, single degree-of-freedom systems. Each of these systems may be identified as a single-input/single-output nonlinear system with feedback and frequency-dependent coefficients. For the first of these systems, the flap motion is the input and the airfoil plunge displacement is the output. The second system has the flap motion as input and the airfoil pitching displacement as output. The nonlinear restoring force in Eq. (3) provides the feedback loop, and the frequency dependence of the coefficients is a result of the integral terms describing the unsteady aerodynamics. The system in the pitch degree-of-freedom is illustrated schematically in Fig. 3 and the equivalent reverse multiple input/single-output system is shown in Fig. 4. The equivalent reverse system is obtained by simply reversing the physical input and response. The flap motion becomes the system mathematical response, and the pitch motion becomes the first mathematical input to the system, or $x_1(\tau)$. The second mathematical input to the system in Fig. 4 $x_2(\tau)$, is obtained from the nonlinear term $M(\alpha(\tau))$ in eq. (1).

The system shown in Fig. 4 is equivalent to the system in Fig. 3 but allows the linear and nonlinear frequency response functions to be identified separately. The identification of the two frequency response functions $A_1(\omega)$ and $A_2(\omega)$ shown in Fig. 4 requires replacement of the two correlated input records with two uncorrelated input records as shown in Fig. 5. The first uncorrelated input record in Fig. 5 $u_1(\tau)$, is the same as the first input in Fig. 4 and is given by the airfoil pitch displacement. The second uncorrelated input record, $u_2(\tau)$, is the result obtained by removing the linear effects of the first input from the second input, and may be obtained from the $x_2(\tau)$ of Fig. 4. The process of removing the linear effects of one input from the other is termed "conditioning", and details of the technique used to obtain conditioned inputs may be found in Bendat and Piersol (1993).

The objective of the aeroelastic analysis is to retrieve the linear frequency response function designated as $A_1(\omega)$ in Fig. 4 which may be used to obtain system modal frequency and damping values. The linear frequency response function$A_1(\omega)$ in the reverse system is the reciprocal of the linear frequency response function for the "forward" system. The relationships that are required to obtain this function from the nonlinear system response are as follows:

$$L_1(\omega) = \frac{S_{1y}(\omega)}{S_{11}(\omega)}, \quad L_2(\omega) = \frac{S_{2y.1}(\omega)}{S_{22.1}(\omega)}, \quad A_2(\omega) = L_2(\omega), \quad A_1(\omega) = L_1(\omega) - \frac{S_{12}(\omega)}{S_{11}(\omega)} A_2(\omega), \tag{5}$$

where the A and L functions are the frequency response relationships shown in Figs. 4 and 5 while the S functions are the cross and auto-spectral densities between the two mathematical inputs and the mathematical output. The conditioned auto- and cross-spectra in the expression for $L_2(\omega)$ may be calculated as follows:

$$S_{2y.1}(\omega) = S_{2y}(\omega) - \frac{S_{1y}(\omega)}{S_{11}(\omega)} S_{21}(\omega), \quad S_{22.1}(\omega) = S_{22}(\omega) - \left|\frac{S_{12}(\omega)}{S_{11}(\omega)}\right|^2 S_{11}(\omega). \tag{6}$$

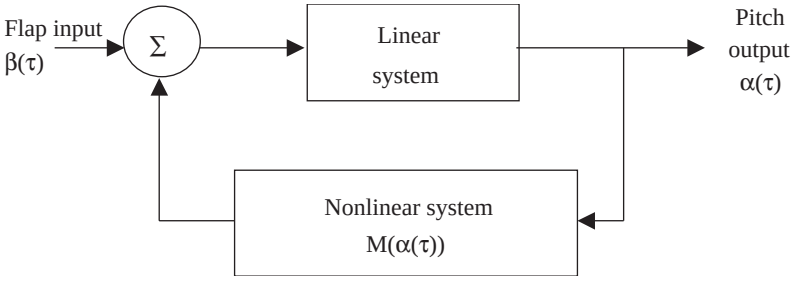

Fig. 3. Single-input/single-output nonlinear model with feedback equivalent to the aeroelastic system in the pitch degree-of-freedom.

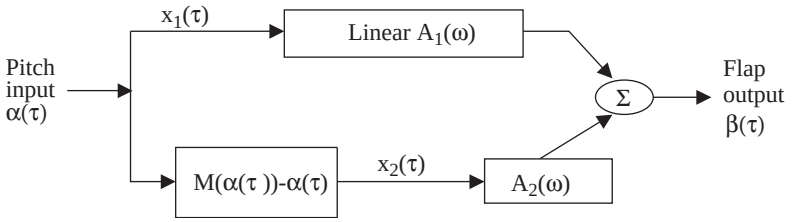

Fig. 4. Reverse single-input/single-output nonlinear system equivalent to Fig. 3.

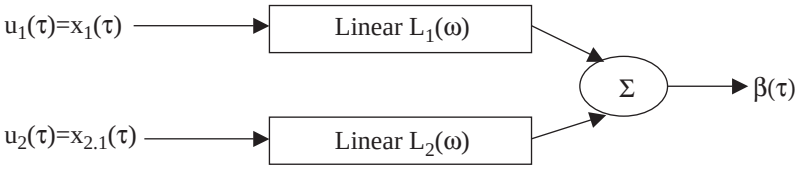

Fig. 5. Multiple-input/single-output linear system with uncorrelated inputs equivalent to Figs. 3 and 4.

3.2. Nonlinear frequency response curve

In terms of equations (5) and (6), the first mathematical input is the pitch displacement time history, and the mathematical output is the flap motion time history as follows:

$$x_1(\tau) = \alpha(\tau), \quad y(\tau) = \beta(\tau).$$

In order to obtain a time history for the second mathematical input, $x_2(\tau)$ of Fig. 4 a function must be assumed for the restoring force term, $M(\alpha(\tau))$ in Eq. (3). For the results shown below, the second mathematical input was obtained from the pitch displacement using Eq. (1), where

$$x_2(\tau) = M(\alpha(\tau)) - \alpha(\tau). \tag{7}$$

The overall nonlinear frequency response function for the reverse system, $L_1(\omega)$, is obtained from the pitch ($x_1(\tau)$) and flap ($y(\tau)$) time-histories using the first of Eq. (5). The frequency response curve obtained for the reverse system is the inverse of the curve normally used for modal analysis, where the peaks in the response curve indicate the modal resonance. In the reverse system frequency response curve, the resonant peaks are minimums and are seen as dips in the curve at the modal natural frequencies. The resulting nonlinear curve for an airspeed equivalent to 64% of the linear flutter speed is plotted in Fig. 6. Analytical values for the reverse linear frequency response function, $A_1(\omega)$, are plotted for comparison. From this example, it is evident that the presence of the structural nonlinearity results in considerable distortion of the frequency response curve. It is apparent that the nonlinear contribution to the frequency response, as obtained directly from the nonlinear data, results in a curve that cannot be used to obtain accurate estimates for system modal frequency and damping. Figs. 7 and 8 compare the first and second mode natural frequencies, respectively, obtained from the linear and nonlinear frequency response curves. The use of the last of Eq. (5) allows this nonlinear

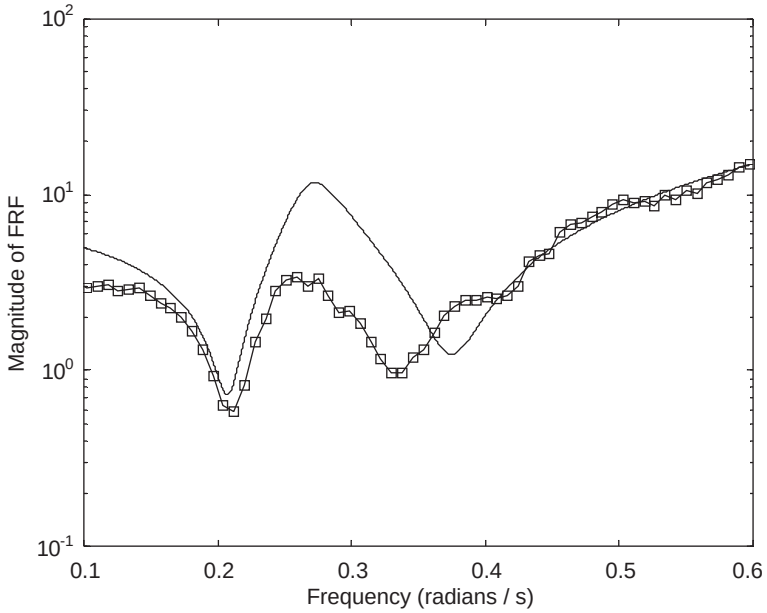

Fig. 6. Frequency response curves for the reverse aeroelastic system at $U/U^* = 0.69$: —□—, frequency response function obtained from nonlinear pitch response; ——, linear frequency response function obtained analytically.

contribution to be removed from the frequency response and the linear frequency response curve to be "recovered" from the nonlinear data.

3.3. "Recovering" the linear frequency response curve

Fourier transforms of the two inputs and the output for the reverse system are obtained and used to calculate the auto- and cross-spectral density functions as follows:

$$S_{11}(\omega) = X_1(\omega)X_1^*(\omega), \quad S_{22}(\omega) = X_2(\omega)X_2^*(\omega), \quad S_{12}(\omega) = \frac{X_1^*(\omega)X_2(\omega)}{X_1^*(\omega)X_1(\omega)}, \quad S_{21}(\omega) = S_{12}^*(\omega),$$

$$S_{1y}(\omega) = \frac{X_1^*(\omega)X_y(\omega)}{X_1^*(\omega)X_1(\omega)}, \quad S_{y1}(\omega) = S_{1y}^*(\omega), \quad S_{2y}(\omega) = \frac{X_2^*(\omega)X_y(\omega)}{X_2^*(\omega)X_2(\omega)}, \quad S_{y2}(\omega) = S_{2y}^*(\omega),$$

where * denotes the complex conjugate. The above expressions may be substituted into equations (5) and (6) to obtain the reverse linear frequency response function, $A_1(\omega)$.

Fig. 9 presents the results for the nonlinear response shown in Fig. 6. In this case, the reverse nonlinear dynamic analysis successfully recovers the linear frequency response curve from the nonlinear data. Similar results were obtained for a number of airspeeds between 69% and 95% of the linear flutter speed, as exemplified by the results of Fig. 10 at 86% of the flutter speed.

3.4. Sensitivity of nonlinear term

The successful application of this technique to the analysis of data from a nonlinear aeroelastic system depends on the accuracy of the mathematical model used to represent the nonlinear input, $x_2(\tau)$. The results shown in Fig. 9 were obtained using the expression for $M(\alpha(\tau))$ from Eq. (1). In other words, the nonlinear input variable is "estimated" exactly as the term that appears in the numerical simulation. Although it may be argued that this considerably restricts the application of this method to aeroelastic test data, it may be assumed that in the case of a similar structural nonlinearity within an aeroelastic system, the structural restoring force could be measured and the function $x_2(\tau)$ determined by curve fitting to experimental data.

In order to test the sensitivity of this method to the choice of $x_2(\tau)$ in Eq. (7), two alternate mathematical expressions were used to approximate the restoring moment function, $M(\alpha(\tau))$. The reverse linear frequency response function was obtained from the nonlinear system response for each of the approximations and compared to the results obtained for

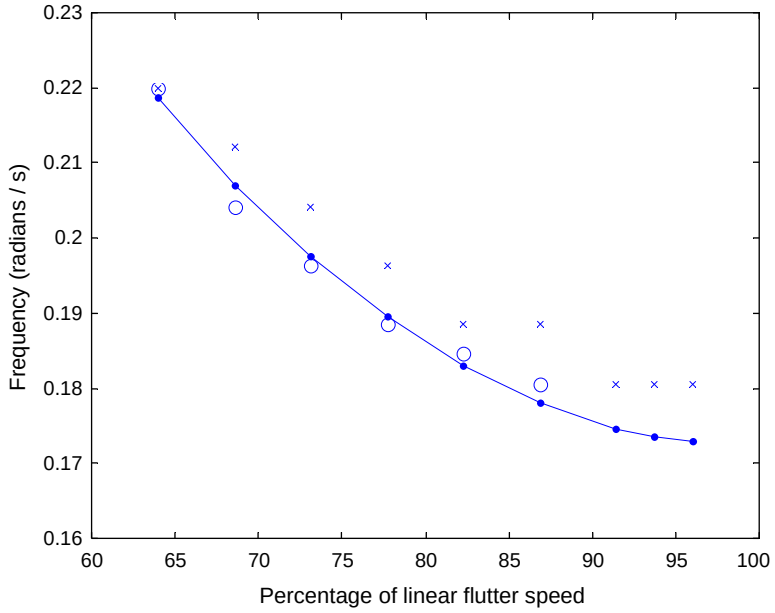

Fig. 7. Variation of first mode natural frequencies with airspeed: ——, linear frequency response function; ×, nonlinear frequency response function; ○, recovered linear frequency response function.

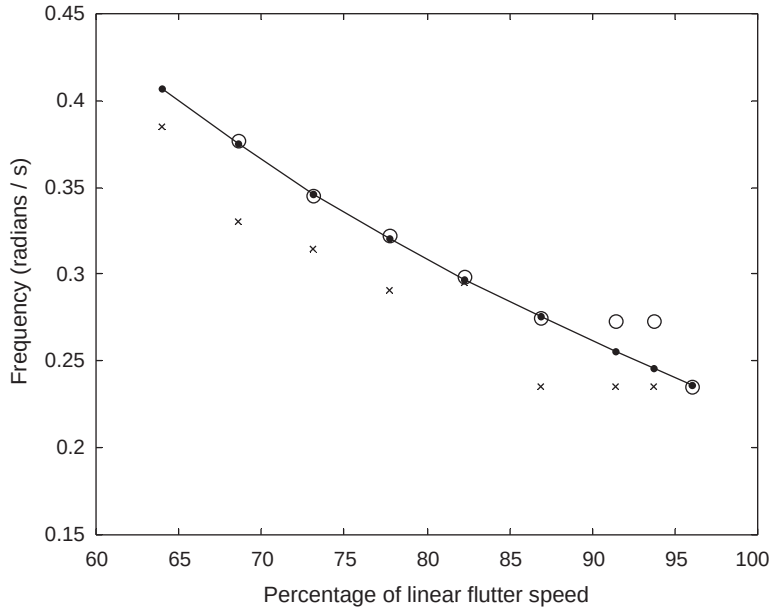

Fig. 8. Variation of second mode natural frequencies with airspeed: ——, linear frequency response function; ×, nonlinear frequency response function; ○, recovered linear frequency response function.

the exact expression in Eq. (1). In the first case, the restoring moment is approximated as a discontinuous function, similar to the function described by Eq. (1), except that the transitions between the linear portions of the curve are not continuous. $M(\alpha(\tau))$ is described by the following expression:

$$M(\alpha(\tau)) = \begin{cases} M_0 + \alpha(\tau) - \alpha_f & \text{for } \alpha \le \alpha_f, \\ M_0 & \text{for } \alpha_f \le \alpha(\tau) \le \alpha_f + \delta, \\ \alpha(\tau) - \alpha_f - \delta + M_0 & \text{for } \alpha(\tau) \ge \alpha_f + \delta. \end{cases}$$

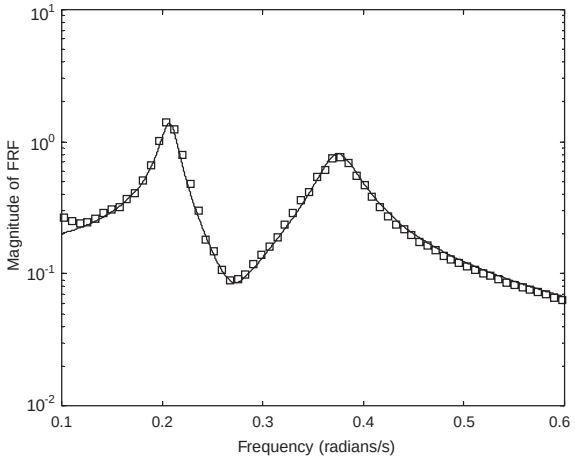

Fig. 9. Comparison between direct frequency response curve recovered from nonlinear system and analytical curve for $U/U^* = 0.69$: —□—, frequency response function recovered from nonlinear pitch response; ——, linear frequency response function obtained analytically.

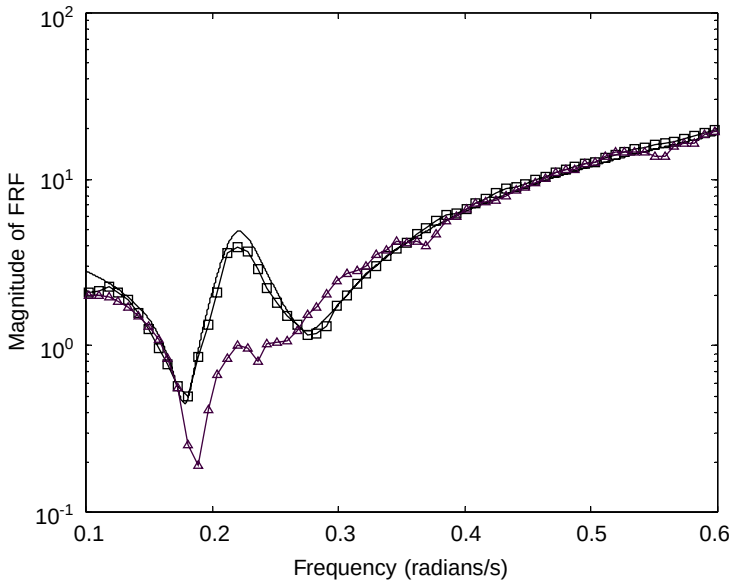

Fig. 10. Comparison between reverse frequency response curves for the nonlinear system and the analytical curve for the linear system at $U/U^* = 0.86$. —△—, frequency response function obtained from nonlinear pitch response; —□—, linear frequency response function recovered from nonlinear curve; ——, analytical linear frequency response function.

In the second case, the restoring moment is approximated as a cubic function of $\alpha(\tau)$:

$$M(\alpha(\tau)) = A\alpha(\tau) + B\alpha^3(\tau),$$

A and B are constants, and the application of the reverse multiple-input/single-output reverse analysis method does not require specific values be assigned for these two constants.

The recovered linear transfer functions obtained for the same nonlinear system response, but using the above two assumptions for the nonlinear restoring force, are shown in Fig. 11 for $U = 3.0$, or 69% of the linear flutter speed. These results are typical of the results obtained at other airspeeds. The discontinuous approximation yields exactly the same results as the exact expression, while the cubic function fails to retrieve a useful estimate of the linear frequency response. This implies that the frequency content of the system response resulting from a discontinuous nonlinearity is

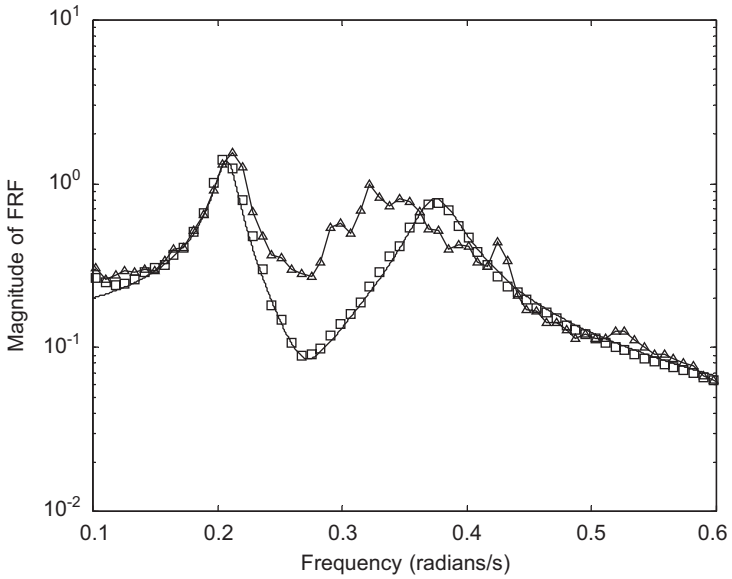

Fig. 11. Linear frequency response curves recovered from the nonlinear data using a discontinuous function and a cubic function approximation for the nonlinear restoring moment in the pitch direction at $U/U^* = 0.69$. —△—, cubic estimate; —□—, discontinuous function; ——, analytical curve.

not the same as that from a cubic nonlinearity, and that the cubic approximation of a discontinuous nonlinearity may be inaccurate in the frequency domain.

4. Discussion

In addition to the sensitivity of this method to the mathematical description of the nonlinear term, the results are also sensitive to the input or forcing function. Oscillating the flap at a scheduled frequency and amplitude provides the excitation to the aeroelastic system. In this study, the equation describing the flap motion is the sum of 500 individual sine waves at random frequencies and is meant to provide a flat frequency content band-limited between 0.1 and 1 rad/s. In fact, the frequency content varies from one simulation to the next, and if there is not sufficient amplitude in the input signal at a given frequency, the frequency response function at that frequency may contain excessive error, particularly in the area of the modal natural frequencies. Running the program for a number of different sets of random frequencies at the input, and averaging the results to obtain a smoother curve may overcome this problem. The use of a random excitation force rather than a deterministic function of a number of different sine waves is also a potential solution, but may not be used with a numerical integration method that requires continuous derivatives of the forcing function.

5. Conclusion

The results presented in this paper suggest the following conclusions regarding the use of the reverse multiple-input/single-output nonlinear method for the analysis of the structurally nonlinear aeroelastic system.

1. The structurally nonlinear aeroelastic system frequency response function, when calculated directly using the nonlinear system input and output time-histories, is significantly distorted when compared to the frequency response function for the equivalent linear system.
2. The use of the reverse multiple-input/single-output nonlinear analysis method allows the recovery of the frequency response function for the equivalent linear system from the nonlinear input and output time-histories.
3. The success of the method is sensitive to the mathematical description of the structural nonlinearity as a function of the aeroelastic system output variable. The mathematical description must adequately represent the actual system nonlinear term.

4. The frequency content of the input or exciting force to the aeroelastic system must have a reasonably flat frequency content for the method to succeed.

Appendix A

Expressions for $f_1(\tau)$ and $f_2(\tau)$ in Eq. (4) are:

$$f_1(\tau) = -m_3\beta''''(\tau) - m_6\beta'''(\tau) - m_9\beta''(\tau) - m_{12}\beta'(\tau) - m_{15}\beta(\tau),$$

$$f_2(\tau) = -\frac{bd}{U^2}M(\alpha(\tau)) - \frac{(b+d)}{U^2}M'(\alpha(\tau)) - \frac{M''(\alpha(\tau))}{U^2} - n_3\beta''''(\tau) - n_6\beta'''(\tau) - n_9\beta''(\tau) - n_{12}\beta'(\tau) - n_{15}\beta(\tau).$$

The coefficients m_i and n_i in Eq. (4) are:

$$m_1 = 1 + \frac{1}{\mu}, \quad m_2 = x_\alpha - \frac{a_h}{\mu},$$

$$m_4 = 2\zeta_\xi\frac{\bar{\omega}_\xi}{U} + (b+d)\left(1+\frac{1}{\mu}\right) + \frac{2}{\mu}(1-a-c),$$

$$m_5 = \frac{1}{\mu} + (b+d)\left(x_\alpha - \frac{a_h}{\mu}\right) + \frac{2}{\mu}(0.5-a_h)(1-a-c),$$

$$m_7 = \left(\frac{\bar{\omega}_\xi}{U}\right)^2 + bd\left(1+\frac{1}{\mu}\right) + 2(b+d)\zeta_\xi\frac{\bar{\omega}_\xi}{U} - \frac{2}{\mu}(ad+cb-b-d),$$

$$m_8 = bd\left(x_\alpha - \frac{a_h}{\mu}\right) + \frac{(b+d)}{\mu} + \frac{2}{\mu}(1-a-c) - \frac{2}{\mu}(0.5-a_h)(ad+bc-b-d),$$

$$m_{10} = 2bd\zeta_\xi\frac{\bar{\omega}_\xi}{U} + (b+d)\left(\frac{\bar{\omega}_\xi}{U}\right)^2 + \frac{2}{\mu}bd,$$

$$m_{11} = \frac{bd}{\mu} - \frac{2}{\mu}(ad+cb-b-d) + \frac{2}{\mu}bd(0.5-a_h),$$

$$m_{13} = bd\left(\frac{\bar{\omega}_\xi}{U}\right)^2, \quad m_{14} = \frac{2bd}{\mu},$$

$$n_1 = \frac{1}{r_\alpha^2}\left(x_\alpha - \frac{a_h}{\mu}\right), \quad n_2 = \frac{1}{\mu r_\alpha^2}\left(\mu r_\alpha^2 + \frac{1}{8} + a_h^2\right),$$

$$n_4 = \frac{x_\alpha}{r_\alpha^2}(b+d) - \frac{a_h}{\mu r_\alpha^2}(b+d) - \frac{2}{\mu r_\alpha^2}(0.5+a_h)(1-a-c),$$

$$n_5 = \frac{2\zeta_\alpha}{U} + \frac{(0.5-a_h)}{\mu r_\alpha^2} + \frac{(b+d)}{\mu r_\alpha^2}\left(\mu r_\alpha^2 + \frac{1}{8} + a_h^2\right) - \frac{2}{\mu r_\alpha^2}(0.5+a_h)(1-a-c)(0.5-a_h),$$

$$n_7 = \frac{bdx_\alpha}{r_\alpha^2} - \frac{bda_h}{\mu r_\alpha^2} - \frac{2}{\mu r_\alpha^2}(0.5+a_h)(b+d-ad-bc),$$

$$n_8 = \frac{bd}{\mu r_\alpha^2}\left(\mu r_\alpha^2 + \frac{1}{8} + a_h^2\right) + \frac{2}{\mu}(b+d)\zeta_\alpha + \frac{(b+d)}{\mu r_\alpha^2}(0.5-a_h) - \frac{2}{\mu r_\alpha^2}(0.5+a_h)(0.5-a_h)(b+d-ad-bc) - \frac{2}{\mu r_\alpha^2}(0.5+a_h)(1-a-c),$$

$$n_{10} = -\frac{2bd}{\mu r_\alpha^2}(0.5+a_h),$$

$$n_{11} = \frac{2bd}{U}\zeta_\alpha + \frac{bd}{\mu r_\alpha^2}(0.5 - a_h) - \frac{2bd}{\mu r_\alpha^2}(0.5 + a_h)(0.5 - a_h) - \frac{2}{\mu r_\alpha^2}(0.5 + a_h)(b + d - ad - bc),$$

$$n_{13} = 0, \quad n_{14} = -\frac{2bd}{\mu r_\alpha^2}(0.5 + a_h).$$

References

Alighanbari, H., Lee, B.H.K., 2003. Analysis of nonlinear aeroelastic signals. Journal of Aircraft 40, 552–558.

Alighanbari, H., Price, S.J., 1996. The post-Hopf bifurcation response of an airfoil in incompressible two-dimensional flow. Nonlinear Dynamics 10, 381–400.

Bendat, J.S., Piersol, A.G., 1993. Engineering Applications of Correlation and Spectral Analysis. Wiley, New York.

Bendat, J.S., 1997. Nonlinear System Techniques and Applications. Wiley, New York.

Conner, M.D., Tang, D.M., Dowell, E.H., Virgin, L.N., 1997. Nonlinear behaviour of a typical airfoil section with a control surface freeplay: a numerical and experimental study. Journal of Fluids and Structures 11, 89–109.

Dowell, E., Tang, D., 2002. Nonlinear aeroelasticity and unsteady aerodynamics. AIAA Journal 40, 1697–1707.

Dowell, E., Edwards, J., Strganac, T., 2003. Nonlinear aeroelasticity. Journal of Aircraft 40, 857–874.

Fung, Y.C., 1955. An Introduction to the Theory of Aeroelasticity. Wiley, New York.

Jones, R.T., 1940. The unsteady lift of a wing of finite aspect ratio. NACA Report 681.

Lee, B.H.K., Price, S.J., Wong, Y.S., 1999. Nonlinear aeroelastic analysis of airfoils: bifurcation and chaos. Progress in Aerospace Sciences 35, 205–334.

Lee, B.H.K., Wong, Y.S., 1998. Neural network parameter extraction with application to flutter signals. Journal of Aircraft 35, 165–168.

Marsden, C.C., 2000. Identification of aeroelastic parameters using sweep excitation. m.eng. thesis, McGill University, Montréal, Québec, Canada.

Marsden, C.C., Price, S.J., 2001. Modal damping identification for a structurally nonlinear airfoil using sweep excitation. Proceedings of the 42nd AIAA/ASME/ASCE/AHS/ASC Structures, Structural Dynamics, and Materials Conference and Exhibit, Seattle, pp. 3008–3018

O'Neil, T., Strganac, T.W., 1998. Aeroelastic response of a rigid wing supported by nonlinear springs. Journal of Aircraft 35, 616–622.

Sheta, E.F., Harrand, V.J., Thompson, D.E., Strganac, T.W., 2002. Computational and experimental investigation of limit cycle oscillations of nonlinear aeroelastic systems. Journal of Aircraft 39, 133–141.

Staszewski, W.J., Cooper, J.E., 2002. Wavelet approach to flutter data analysis. Journal of Aircraft 39, 125–132.

Tang, D., Dowell, E.H., 1993. Comparison of theory and experiment for non-linear flutter and stall response of a helicopter blade. Journal of Sound and Vibration 165, 251–276.

Tang, D., Dowell, E.H., Virgin, L.N., 1998. Limit cycle behaviour of an airfoil with a control surface. Journal of Fluids and Structures 12, 839–858.

Zimmerman, N.H., Weissenburger, J.T., 1964. The prediction of flutter onset speed based on flight testing at subcritical speeds. Journal of Aircraft 1, 190–202.